Synthesis and Characterization of Fe₃O₄@SiO₂ NPs as an Effective Catalyst for the Synthesis of Tetrahydrobenzo[*a*]xanthen-11-ones

Mohammad Ali Ghasemzadeh*

Department of Chemistry, Qom Branch, Islamic Azad University, Qom, I. R. Iran
Department of Organic Chemistry, Faculty of Chemistry,

* Corresponding author: E-mail: Ghasemzadeh@qom-iau.ac.ir

Abstract

In this research, the significant application of Fe₃O₄@SiO₂ core-shell nanoparticles as efficient, green, robust, cost-effective and recoverable nanocatalyst for the multi-component reaction of aldehydes, 2-naphthol and dimedone has been developed in aqueous ethanol media under reflux conditions. In the presented procedure we had avoided to use of hazardous reagents and solvents and therefore this method can be considered as a green alternative pathway in comparison with the previous method. Simple procedure, environmentally benign, excellent yields, short reaction times, simple purification and facile catalyst separation are advantages of this protocol. Characterization and structural elucidation of the prepared products have been done on the basis of chemical, analytical and spectral analysis. In addition, the heterogeneous nanoparticles were fully characterized by FT-IR, XRD, EDX, VSM and SEM analysis.

Keywords: Core-shell, nanoparticles, Fe₃O₄@SiO₂, tetrahydrobenzo[*a*]xanthen-11-one, three-component reactions, heterocyclic compounds

1. Introduction

Core-shell nanostructures have aroused considerable interest in the various fields because of their functional attributes, such as great scattering and stability. Core-shell nanoparticles are perfect complex systems that involve the benefits of both core and shell to improve chemical and physical properties. Surface modification of nanoparticles has certainly attracted great attention in the multidisciplinary areas of organic chemistry and nanotechnology.[1,2]

Recently, magnetite Fe₃O₄ nanoparticles, (Fe₃O₄ NPs) have been used extensively as inorganic cores for the preparation of inorganic/organic core/shell nanocomposites, due to their significant applications in various chemical, biomedical and industrial scopes.[3]

In particular, functionalized magnetite nanocatalysts show not only excellent catalytic performance but also have a good grade of high chemical stability in the many organic transformations.[4] In addition, magnetite-supported nanocatalysts can be easily separated using an external magnet and their catalytic activity remains after several reaction cycles.[5]

Silica-coating of nanoparticles is an ideal surface modifier, due to its high stability, bio-adaptability, being non-poisonous, and easily attached to diverse functional groups. The nanostructures involving silica-coated magnetite nanoparticles (Fe₃O₄@SiO₂ core-shell nanoparticles) as catalyst with many reactive portions, acidic features and high surface area do not only supply high chemical stability but are also appropriate for the many functionalizations.[6,7]

Recently, functionalized magnetite nanoparticles were used as efficient catalytic systems in many chemical transformations including synthesis of α-amino nitriles,[8] 1,1-diacetates from aldehydes,[9] diazepine derivatives,[10] indazolo[2,1-*b*]phthalazine-triones and pyrazolo[1,2-*b*]phthalazine-diones,[11] 3,4-dihydropyrimidin-2(1*H*)-ones,[12] 2-amino-4*H*-chromen-4-yl phosphonates,[13] 1,4-dihydropyridines[14] and pyrrole synthesis.[15] In addition, a series of organic reactions such as Knoevenagel condensation/Michael addition,[16] Suzuki/Heck cross-coupling,[17] asymmetric aldol reaction,[18] Suzuki coupling,[19] asymmetric hydrogenation of aromatic ketones,[20] acetalization reaction,[21] Ritter reaction,[22] cyanosilylation of carbonyl

compounds,[23] Henry reaction,[24] enantioselective direct-addition of terminal alkynes to imines[25] have been done using functionalized nanostructures.

The multi-component reactions (MCRs) are appearing as valuable tools to produce compound libraries of small molecules for potential applications in medicinal and pharmaceutical chemistry.[26] MCRs often conform to the aims of green chemistry related to economy of the reaction steps as well as the many precise principles of desirable organic synthesis.[27] Because of their advantages, including facile performance, being environmentally benign, fast and atom economic, MCRs have caused a great interest in relation to combinatorial chemistry.

Benzoxanthens are known, due to their numerous occurence in nature and extensive range of pharmacological and therapeutic properties, including antiviral,[28] antibacterial,[29] anti-inflammatory,[30] and other bioorganic characteristics.[31] In addition, these compounds are applied widely in laser technologies,[32] dyes,[33] and as pH-sensitive fluorescent materials for visualization of biomolecules.[34]

12-Aryl-8,9,10,12-tetrahydrobenzo[a]xanthen-11-ones are a class of benzoxanthen derivatives which can be prepared via three-component reaction of aldehydes, 2-naphthol and cyclic 1,3-dicarbonyl compounds. Because of the importance of the structures of these compounds we observe a lot of approaches in the literature for the preparation of benzo[a]xanthen-11-one derivatives.

Three-component condensation of aldehydes, 2-naphthol and cyclic 1,3-dicarbonyls has been carried out using diverse catalysts, such as: biodegradable ionic liquid [DDPA][HSO$_4$],[35] HClO$_4$-SiO$_2$,[36] [Py(HSO$_4$)$_2$],[37] cyanuric chloride,[38] iodine,[39] tetradecyltrimethylammonium bromide (TTAB),[40] sulfamic acid,[41] H$_2$SO$_4$,[42] InCl$_3$ or P$_2$O$_5$,[43] molecular iodine,[44] and Fe$_3$O$_4$/CS-Ag NPs.[45]

In the context of our interest on sustainable approaches in the preparation of heterocyclic compounds and in continuation of our interest towards the advancement of effective and environmentally friendly nanoca-

talysts in organic synthesis,[46–52] we now wish to report a green and efficient method for the preparation of 12-aryl-8,9,10,12-tetrahydrobenzo[a]xanthen-11-ones by MCRs using Fe$_3$O$_4$@SiO$_2$ core-shell nanoparticles as robust, environmentally benign and resuabale catalyst with acidic properties.

2. Results and Discussion

In the preliminary experiments Fe$_3$O$_4$ and Fe$_3$O$_4$@SiO$_2$ nanoparticles were prepared and characterized by EDX, XRD, SEM, IR and VSM analysis. The chemical purity of the samples as well as their stoichiometry was tested by energy dispersive X-ray spectroscopy (EDAX) studies. The EDAX spectrum given in Figure 1a shows the presence of Fe and O as the only elementary components of Fe$_3$O$_4$ NPs. In addition, as shown in Figure 1b, the Si peak clearly confirms the presence of SiO$_2$ groups on the Fe$_3$O$_4$@SiO$_2$ core-shell nanoparticles.

The X-ray diffraction patterns of Fe$_3$O$_4$ and Fe$_3$O$_4$@SiO$_2$ are shown in Figure 2. The position and relative intensities of all peaks confirm well with standard XRD pattern of Fe$_3$O$_4$ with P63mc group (JCDPS No. 75-0449) indicating retention of the crystalline cubic spinel structure during functionalization of MNPs. Characteristic peak of SiO$_2$ in core shell structure has been hidden under weak peak of Fe$_3$O$_4$ at $2\theta = 30$. The average MNPs core diameter was calculated to be 25 nm from the XRD results by Scherrer's equation, $D = k \lambda / b \cos h$ where k is a constant (generally considered as 0.94), λ is the wavelength of Cu Kα (1.54 Å), b is the corrected diffraction line full-width at half-maximum (FWHM), and h is Bragg's angle.

In order to study the morphology and particle size of Fe$_3$O$_4$ nanoparticles, SEM image of Fe$_3$O$_4$ nanoparticles is presented in Figure 3a. These results show that spherical Fe$_3$O$_4$ NPs were obtained with an average diameter of about 20–30 nm as confirmed by X-ray line broadening
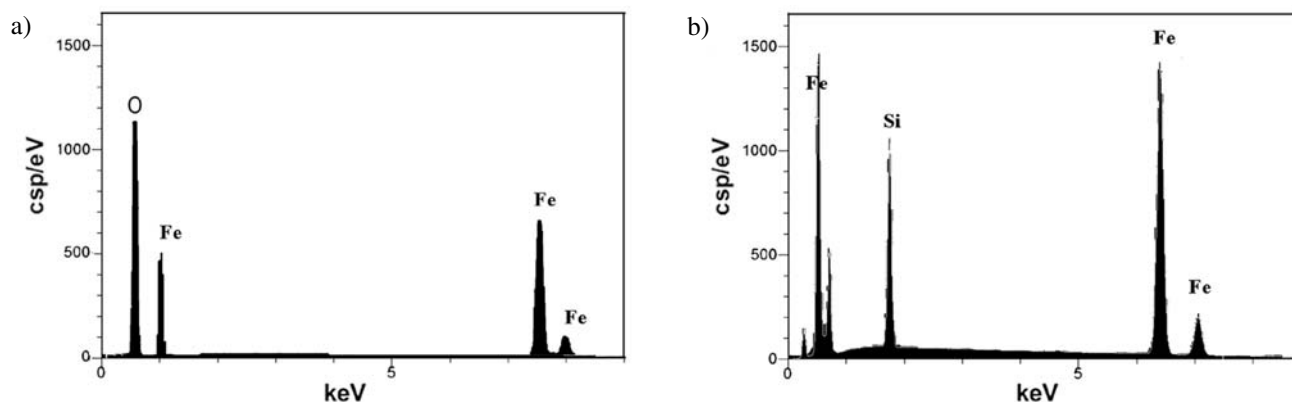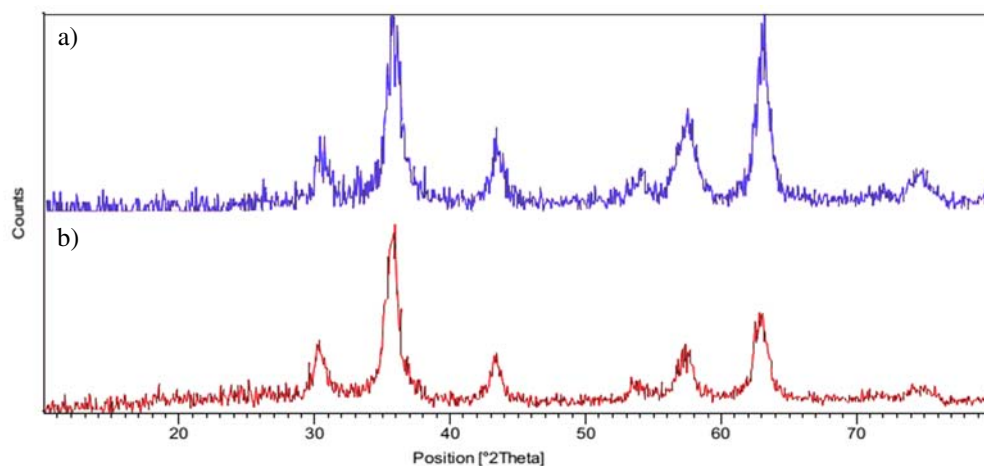

Figure 1. The EDX spectra of Fe$_3$O$_4$ (a) and Fe$_3$O$_4$@SiO$_2$ NPs (b)

Figure 2. XRD patterns of Fe_3O_4 NPs (a) and $Fe_3O_4@SiO_2$ NPs (b)

analysis. As shown in Figure 3b, $Fe_3O_4@SiO_2$ nanoparticles still keep the morphological properties of Fe_3O_4 except for a slightly larger particle size and smoother surface, where silica uniformly coated the Fe_3O_4 particles to form silica shell, as compared to the Fe_3O_4.

Figure 4 shows the FT-IR spectra for the samples of Fe_3O_4 NPs and $Fe_3O_4@SiO_2$ microspheres catalysts. For the bare magnetic nanoparticles (Figure 4a), the vibration band at 575 cm^{-1} is the typical IR absorbance induced by structure Fe–O vibration. The absorption band at 1072 cm^{-1} observed on $Fe_3O_4@SiO_2$ nanoparticles can be ascribed to the stretching and deformation vibrations of Si-

O_2, reflecting the coating of silica on the magnetite surfaces (Figure 4b).

The magnetic properties of the samples containing a magnetite component were studied by a vibrating sample magnetometer (VSM) at 300 K. Figure 5 shows the absence of hysteresis phenomenon and indicates that all of the products exhibit superparamagnetism at room temperature. The saturation magnetization values for Fe_3O_4 (a), $Fe_3O_4@SiO_2$ (b) were 46.32 and 38.16 emu/g, respectively. These results indicated that the magnetization of Fe_3O_4 decreased considerably with introducing the SiO_2 shell.
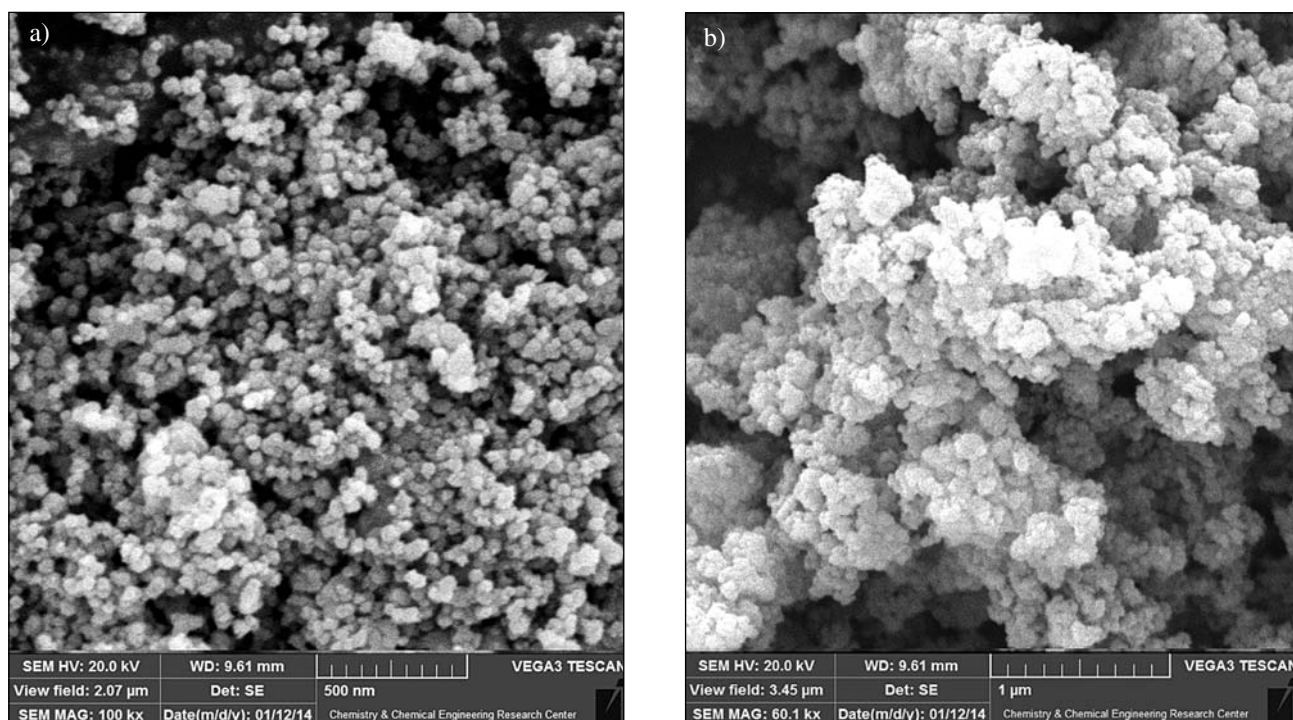

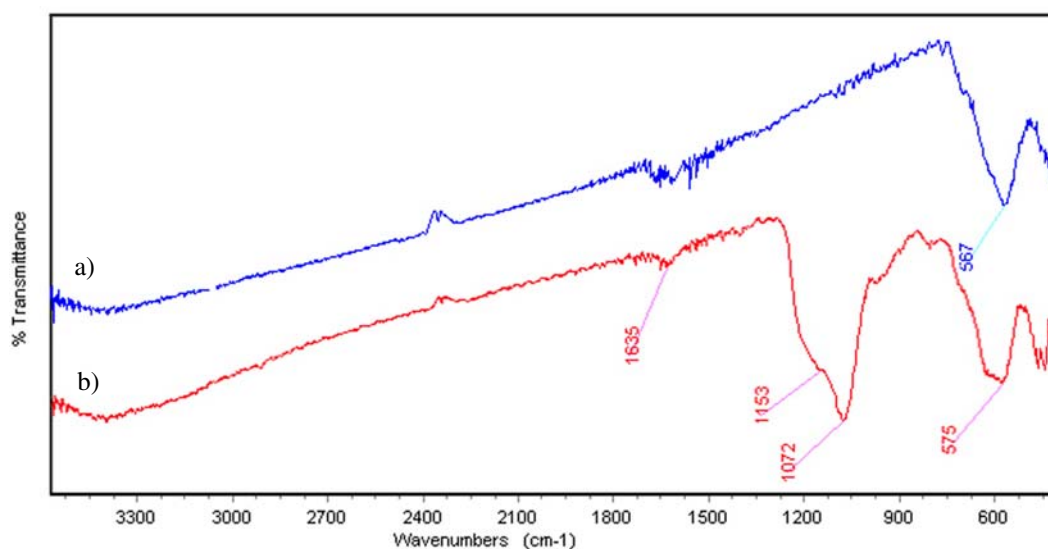**Figure 3.** The SEM images of Fe_3O_4 (a) and $Fe_3O_4@SiO_2$ NPs (b)

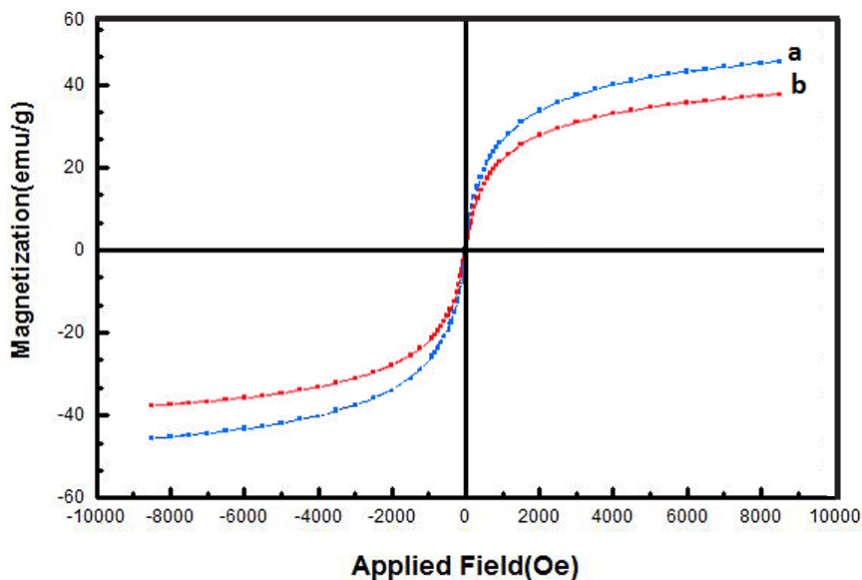**Figure 4.** The comparative FT-IR spectra of Fe_3O_4 (a) and $Fe_3O_4@SiO_2$ (b) nanoparticles

Figure 5. Magnetization curves for the prepared of Fe_3O_4 (a) and $Fe_3O_4@SiO_2$ NPs (b)FT

In the preliminary experiments, in order to determine the optimized reaction conditions the reaction of 4-nitrobenzaldehyde (1 mmol), 2-naphthol (1 mmol) and dimedone (1 mmol) was selected as a model reaction and the reaction conditions were optimized on the base of solvent and catalyst (Scheme 1).

This model study was carried out in the presence of non-polar (Table 1, entries 1, 2), aprotic solvents (Table 1, entries 3, 4) and protic solvents (Table 1, entries 5–8) using 15 mol% of $Fe_3O_4@SiO_2$ nanoparticles. As shown in Table 1 the best result was obtained in H_2O/EtOH (Table 1, entry 8) as the solvent for this multi-component reaction. It seems that the nucleophilic attack of the reactants

can proceed smoothly by hydrogen bonding between water/ethanol and substrates.

Next, we carried out the model reaction in H_2O/EtOH at various temperatures (Table 1, entries 9, 10). As can be seen maximum yield was obtained under reflux conditions (Table 1, entry 8).

The model reaction was also investigated in the absence of the catalyst as well as in the presence of different catalysts (Table 2, entries 2–12). Although in the absence of the catalyst only a trace amount of the product was obtained after 8 h. Many homogenous and heterogeneous catalysts, such as CH_3COOH, $MgSO_4$, NaOH, piperidine, Et_3N, MgO NPs, CaO NPs, CuO NPs, AgI
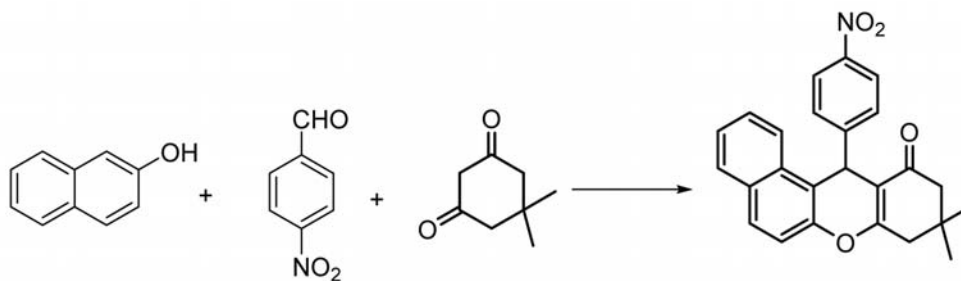
Scheme 1. The model reaction for the prepatation of tetrahydrobenzo[*a*]xanthen-11-one (**4h**)

Table 1. The model study in different solvents using $Fe_3O_4@SiO_2$ NPs.[a]

Entry	Solvent	T/°C	Time/min	Yields[b]/%
1	PhCH$_3$	reflux	160	45
2	CH$_2$Cl$_2$	reflux	150	35
3	DMF	reflux	120	60
4	CH$_3$CN	reflux	100	55
5	EtOH	reflux	65	85
6	CH$_3$OH	reflux	70	80
7	H$_2$O	reflux	75	75
8	H$_2$O/EtOH	reflux	45	94
9	H$_2$O/EtOH	50°C	120	60
10	H$_2$O/EtOH	r.t.	240	40

[a] Reaction conditions: molar ratio of aldehyde, 2-naphthol and dimedone (1:1:1), $Fe_3O_4@SiO_2$ (15 mol %); [b] Isolated yields

Table 2. The model study for the synthesis of xanthene 4h by various catalysts.[a]

Entry	Catalyst	Time (min)	Yields[b]/%
1	none	480	trace
2	CH$_3$COOH (15 mol%)	50	75
3	MgSO$_4$ (15 mol%)	70	44
4	NaOH (15 mol%)	180	30
5	Piperidine (15 mol%)	150	35
6	Et$_3$N (15 mol%)	140	38
7	MgO NPs (15 mol%)	90	60
8	CaO NPs (15 mol%)	100	50
9	CuO NPs (15 mol%)	75	70
10	AgI NPs (15 mol%)	65	75
11	Fe$_3$O$_4$ NPs (15 mol%)	55	80
12	Fe$_3$O$_4$@SiO$_2$ NPs (15 mol%)	45	94
13	Fe$_3$O$_4$@SiO$_2$ NPs (10 mol%)	45	94
14	Fe$_3$O$_4$@SiO$_2$ NPs (8 mol%)	45	94
15	Fe$_3$O$_4$@SiO$_2$ NPs (5 mol%)	45	94
16	Fe$_3$O$_4$@SiO$_2$ NPs (2 mol%)	60	82

[a] Reaction conditions: molar ratio of aldehyde, 2-naphthol and dimedone (1:1:1); in water/ethanol under reflux conditions; [b] Isolated yield.

NPs, Fe_3O_4 NPs and $Fe_3O_4@SiO_2$ NPs, were used to investigate the model reaction in H$_2$O/EtOH as solvent under reflux conditions (15 mol% of each catalyst was used separately).

The summarized results in Table 2 show that most of the Brønsted and Lewis acids could carry out the model reaction. However, we found that $Fe_3O_4@SiO_2$ NPs (Table 2, entry 12) gave the best results in comparison with other catalysts in three-component reaction of 4-nitrobenzaldehyde, 2-naphthol and dimedone.

The increased catalytic activity of silica-coated magnetite nanoparticles in regard to the other catalysts is related to a high surface-area-to-volume ratio of supported magnetite nanoparticles which provide enormous driving force for diffusion.

Next, the effect of different concentrations of catalyst was evaluated using various amounts of $Fe_3O_4@SiO_2$ NPs including 2 mol%, 5 mol%, 8 mol%, 10 mol% and 15 mol%. We observed that 5 mol% of $Fe_3O_4@SiO_2$ NPs afforded product with the best results and it was enough for a complete progress of the reaction (Table 2).

We investigated the scope and limitations of three-component reactions of aldehydes, 2-naphthol and dimedone under the optimized conditions. So we carried out synthesis of 12-aryl-8,9,10,12-tetrahydrobenzo[*a*]xant-

hen-11-one derivatives by use of various structures of aldehydes in the presence of $Fe_3O_4@SiO_2$ core shell NPs (Scheme 2, Table 3).

A number of experiments have been performed and therefore we synthesized a series of tetrahydrobenzo[*a*]xanthen-11-ones in excellent yields and un short reaction times. As can be seen from Table 3, aromatic aldehydes bearing electron-withdrawing groups, such as F and Cl (Table 3, Entries 3, 4) reacted easier and faster than those with electron-releasing groups, such as Me and OMe as expected. Also the synthesis of 12-aryl-8,9,10,12-tetrahydrobenzo[*a*]xanthen-11-one derivatives using sterically hindered aromatic aldehydes required longer reaction times.

A plausible mechanism for the synthesis of 12-aryl-8,9,10,12-tetrahydrobenzo[*a*]xanthen-11-ones using $Fe_3O_4@SiO_2$ NPs is shown in Scheme 3. It is likely that $Fe_3O_4@SiO_2$ NPs act as a Lewis acid and increase the electrophilicity of the carbonyl groups on the
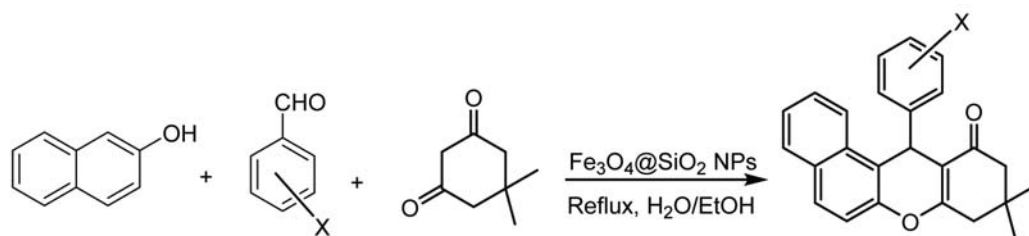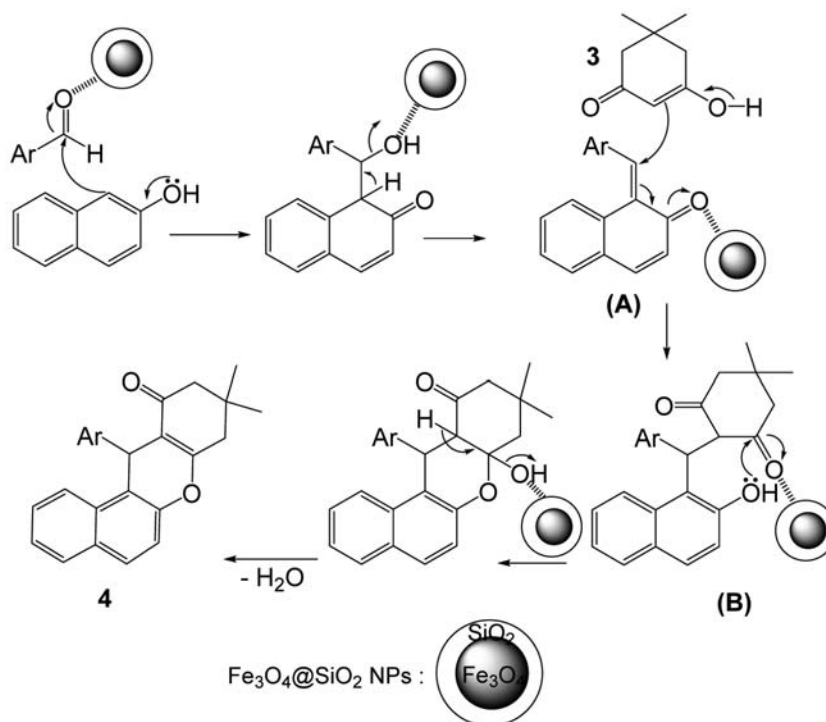
Scheme 2. Preparation of tetrahydrobenzo[*a*] xanthen-11-ones catalyzed by Fe$_3$O$_4$@SiO$_2$ NPs

Table 3. Synthesis of tetrahydrobenzo[*a*]xanthen-11-ones catalyzed by Fe$_3$O$_4$@SiO$_2$ NPs.

Entry	Aldehyde (X)	Products 4	Time(min)/ Yield^a(%)	M.p./ °C^{ref}
1	C$_6$H$_5$	**4a**	50/87	151–153[41]
2	2-OMe	**4b**	55/86	166–168[41]
3	4-OMe	**4c**	52/88	203–205[41]
4	4-OH	**4d**	50/90	212–213[41]
5	3-Me	**4e**	52/86	176–177[37]
6	4-Me	**4f**	48/88	175–177[42]
7	3-NO$_2$	**4g**	52/90	170–172[41]
8	4-NO$_2$	**4h**	45/94	185–187[41]
9	4-Cl	**4i**	40/92	181–182[41]
10	2,4-Cl$_2$	**4j**	55/92	179–181[41]
11	4-Br	**4k**	48/92	181–183[42]
12	4-F	**4l**	45/92	184–185[42]
13	2,4-(OMe)$_2$	**4m**	60/86	226–227
14	2-F	**4n**	51/89	173–174[44]

^{a} Isolated yield; ^{b} New Products.

aldehyde and dimedone by means of a strong coordination bond.

Initially, the nucleophilic addition of aldehydes and 2-naphthol in the presence of Fe$_3$O$_4$@SiO$_2$ NPs as catalyst leads to *ortho*-quinone methides (*o*-QMs) intermediate **A**. Subsequent Michael addition of dimedone with *o*-QM forms intermediate **B** which coordinates to the catalyst to cyclized accompanied by loss of H$_2$O to afford product **4**.

3. Experimental

3. 1. General

Chemicals were of commercial reagent grade and obtained from Merck or Fluka and used without further purification. All products were characterized by comparison of their FT-IR and NMR spectra and physical data with those reported in the literature. All yields refer to the

Scheme 3. Proposed mechanism for the reaction of aldehydes, 2-naphthol and dimedone by Fe$_3$O$_4$@SiO$_2$ NPs

isolated products. Progress of reactions was followed by TLC on silica-gel Polygram SILG/UV 254 plates. IR spectra were run on a Shimadzu FT-IR- 8300 spectrophotometer. NMR spectra were recorded on a Bruker Avance DRX instrument (400 MHz). The elemental analyses (C, H, N) were obtained from a Carlo ERBA Model EA 1108 analyzer. The mass spectra were recorded on a Joel D-30 instrument at an ionization potential of 70 eV. Microscopic morphology of products was visualized by SEM (LEO 1455VP). Powder X-ray diffraction (XRD) was carried out on a Philips diffractometer of X'pert Company with mono chromatized Cu Kα radiation (λ = 1.5406 Å). The compositional analysis was done by energy dispersive analysis of X-ray (EDX, Kevex, Delta Class I). Magnetic properties were obtained on a BHV-55 vibrating sample magnetometer (VSM).

3. 2. Preparation of Fe_3O_4 Nanoparticles

Fe_3O_4 MNPs were prepared according to a previously reported procedure by Hu et al.[53] using the chemical co-precipitation method. Typically, $FeCl_3 \times 6H_2O$ (2.7 g) and $FeCl_2 \times 4H_2O$ (1 g) were dissolved in 100 mL of 1.2 mmol/L aqueous HCl followed by ultrasonic bath for 30 min. Then, 1.25 mol/L aqueous NaOH (150 mL) was added under vigorous stirring and a black precipitate was immediately formed. The resulting transparent solution was heated at 80 °C with rapid mechanical stirring under N_2 atmosphere (scheme 2). After vigorous stirring for 2 h, the black products were centrifuged, filtered out and washed with deionized water and alcohol for several times, and finally dried at 60 °C for 12 h.

3. 3. Preparation of $Fe_3O_4@SiO_2$ Nanoparticles

$Fe_3O_4@SiO_2$ core-shell particles were prepared via modified Stöber sol-gel process.[54] 30 mg as-prepared Fe_3O_4 submicrospheres were ultrasonically dispersed in a solution containing 160 mL ethanol, 40 mL water and 10 mL concentrated ammonia (28 wt%). Then, 0.4 mL TEOS was added dropwise to the solution under sonication, followed by mechanical stirring for 3 h at room temperature.

Subsequently, the resulting particles were separated using a magnet and washed with deionized water and ethanol. This step was repeated several times before drying at 60 °C for 12 h (Scheme 4).

3. 4. General Procedure for the Synthesis of 12-Aryl-8,9,10,12-tetrahydrobenzo [*a*]xanthen-11-ones (4a–n).

A mixture of aldehyde (1 mmol), 2-naphthol (1 mmol), dimedone (1 mmol) and $Fe_3O_4@SiO_2$ NPs (0.014 g, 0.5 mmol, 5 mol%) in 2.5 mL ethanol and 2.5 mL water was refluxed at 80 °C. After completion of the reaction as indicated by TLC, the reaction mixture was cooled to room temperature and then diluted with chloroform (10 mL), the catalyst was recovered by using an external magnet. The solvent was evaporated and the solid obtained was recrystallized using ethanol.

All of the products were characterized and identified with m.p., ^1H NMR, ^{13}C NMR and FT-IR spectroscopy techniques. Spectral data of some of the products are given below.

12-(2,4-Dimethoxyphenyl)-9,9-dimethyl-9,10-dihydro-8*H*-benzo[*a*]xanthen-11(12*H*)-one (4m).

White crystals; m.p. 226–227 °C; ^1H NMR (400 MHz, $CDCl_3$) δ 0.99 (s, 3H, CH_3), 1.14 (s, 3H, CH_3), 2.21–2.31 (m, 2H, CH_2), 2.52 (s, 2H, CH_2), 3.74 (s, 3H, OCH_3), 3.86 (s, 3H, OCH_3), 5.71 (s, 1H, CH), 6.78 (s, 1H, Ar-H), 6.94–7.10 (m, 2H, Ar-H), 7.05–7.35 (d, 1H, Ar-H), 7.53–7.56 (m, 2H, Ar-H), 7.64–7.69 (d, 3H, Ar-H) ppm; ^{13}C NMR (100 MHz, $CDCl_3$) δ 26.7, 29.6, 32.3, 33.6, 41.8, 50.0, 55.6, 59.6, 109.5, 113.5, 115.1, 115.4, 119.3, 128.8, 129.2, 130.8, 131.0, 132.0, 144.1, 148.5, 151.4, 156.0, 156.8, 158.0, 161.8, 163.0, 195.7 ppm; FT-IR (KBr): n 1666 (C=O), 1625 (C=C, Ar), 1197 (C–O) cm^{-1}; MS *m/z*: 414 (M⁺); Anal. Calcd for $C_{27}H_{26}O_4$: C, 78.24; H, 6.32. Found: C, 78.32; H, 6.26%.

12-(2-Fluorophenyl)-9,9-dimethyl-9,10-dihydro-8*H*-benzo[*a*]xanthen-11(12*H*)-one (4n).

White crystals; m.p. 173–174 °C; ^1H NMR (400 MHz, $CDCl_3$) δ 0.99 (s, 3H, CH_3), 1.10 (s, 3H, CH_3),
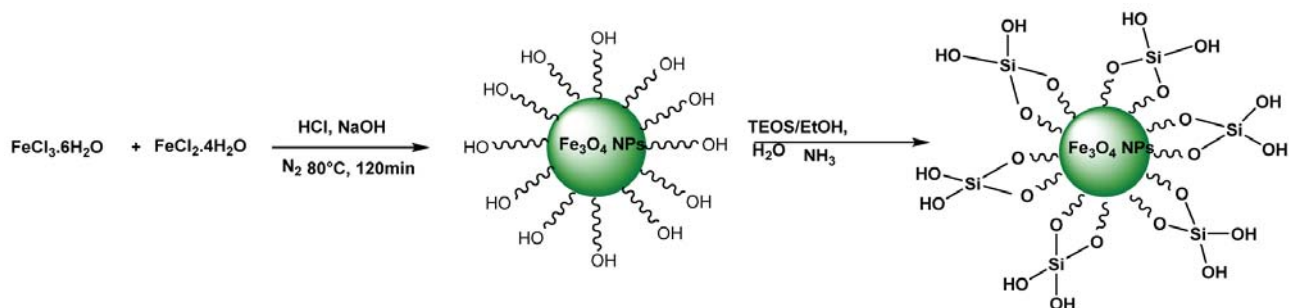
Scheme 4. Preparation steps for fabricating $Fe_3O_4@SiO_2$

2.28–2.32 (m, 2H, CH$_2$), 2.59–2.65 (m, 2H, CH$_2$), 5.97 (s, 1H, CH), 6.77–6.83 (m, 2H, Ar-H), 7.02–7.06 (m, 1H, Ar-H), 7.25–7.28 (m, 2H, Ar-H), 7.33–7.46 (m, 2H, Ar-H), 7.69–7. 75 (m, 2H, Ar-H), 8.28–8.31 (d, 1H, Ar-H) ppm; ^{13}C NMR (100 MHz, CDCl$_3$) δ 26.6, 27.2, 29.6, 32.4, 41.7, 50.0, 114.0, 115.1, 128.1, 129.0, 129.3, 129.6, 129.8, 130.0, 131.3, 131.8, 138.7, 139.6, 142.8, 143.3, 144.9, 150.1, 162.6, 163.3, 196.4 ppm; FT-IR (KBr) n 1663 (C=O), 1517 (C=C, Ar), 1200 (C–O) cm^{-1}; MS *m/z*: 372 (M$^+$); Anal. Calcd for C$_{25}$H$_{21}$FO$_2$: C, 80.62; H, 5.68. Found: C, 80.71; H, 5.61%.

3. 5. Recycling and Reusing of the Catalyst

After completion of the reaction, the reaction mixture was dissolved in chloroform and then the catalyst was separated magnetically. The Fe$_3$O$_4$@SiO$_2$ NPs were washed three to four times with chloroform and ethylacetate and dried at 60 °C for 8 h. The separated catalyst was used for six cycles with a slight decrease in activity as shown in Table 4.

Table 4. Reusability of the Fe$_3$O$_4$@SiO$_2$ nanoparticles[a]

First	Second	Third	Fourth	Fifth	Sixth
		Yield (%)[b]			
94	93	90	89	85	82

[a] Reaction conditions: molar ratio of 4-nitrobenzaldehyde, 2-naphthol, dimedone (1:1:1); in water/ethanol under reflux conditions using recycled Fe$_3$O$_4$@SiO$_2$; [b] Isolated yield.

4. Conclusions

In summary, we have developed a novel and highly efficient method for the one-pot preparation of 14-aryl-14*H*-dibenzo[*a*]xanthene-8,13-dione derivatives by the reaction of β-naphthol, aromatic aldehydes and dimedone in the presence of Fe$_3$O$_4$@SiO$_2$ core-shell nanoparticles as the catalyst. The significant advantages of this methodology are high yields, a cleaner reaction, simple work-up procedure, short reaction times and easy preparation, reusability and handling of the catalyst. In addition, the one-pot nature and the use of heterogeneous solid acid as an eco-friendly catalyst make it an interesting alternative to multi-step approaches.

5. Acknowledgements

6. References

1. T. V. Werne, T. E. Patten, *J. Am. Chem. Soc.* **1999**, *121*, 7409–7410. http://dx.doi.org/10.1021/ja991108l
2. S. G. Kwon, T. Hyeon, *Acc. Chem. Res.* **2008**, *41*, 1696–1709. http://dx.doi.org/10.1021/ar8000537
3. A. Hu, G. T. Yee, W. Lin, *J. Am. Chem. Soc.* **2005**, *127*, 12486–12487. http://dx.doi.org/10.1021/ja053881o
4. G. Chouhan, D. Wang, H. Alper, *Chem. Commun.* **2007**, *45*, 4809–4811. http://dx.doi.org/10.1039/b711298j
5. M. Faraji, Y. Yamini, M. Rezaee, *J. Iran. Chem. Soc.* **2010**, *7*, 1–37.
6. B. G. Wang, B. C. Ma, Q. Wang, W. Wang, *Adv. Synth. Catal.* **2010**, *352*, 2923–2928. http://dx.doi.org/10.1002/adsc.201000508
7. Q. Zhang, H. Su, J. Luo, Y. Wei, *Green Chem.* **2012**, *14*, 201–208. http://dx.doi.org/10.1039/C1GC16031A
8. M. Z. Kassaee, H. Masrouri, F. Movahedi, *Appl. Catal. A-Gen.* **2011**, *395*, 28–33. http://dx.doi.org/10.1016/j.apcata.2011.01.018
9. M. Esmaeilpour, A. R. Sardarian, J. Javidi, *Appl. Catal. A-Gen.* **2012**, *445–446*, 359–367. http://dx.doi.org/10.1016/j.apcata.2012.09.010
10. A. Maleki, *Tetrahedron Lett.* **2013**, *54*, 2055–2059. http://dx.doi.org/10.1016/j.tetlet.2013.01.123
11. A. R. Kiasat, J. Davarpanah, *J. Mol. Catal. A-Chem.* **2013**, *373*, 46–54. http://dx.doi.org/10.1016/j.molcata.2013.03.003
12. F. Zamani, E. Izadi, *Catal. Commun.* **2013**, *42*, 104–108. http://dx.doi.org/10.1016/j.catcom.2013.08.006
13. R. Mohammadi, M. Z. Kassaee, *J. Mol. Catal. A-Chem.* **2013**, *380*, 152–158. http://dx.doi.org/10.1016/j.molcata.2013.09.027
14. M. B. Gawande, V. D. B. Bonifácio, R. S. Varma, I. D. Nogueira, N.Bundaleski, C. Amjad, A. Ghumman, M. N. D. Teodoro, P. S. Branco, *Green Chem.* **2013**, *15*, 1226–1231. http://dx.doi.org/10.1039/c3gc40375k
15. H. Mahmoudi, A. A. Jafari, *ChemCatChem.* **2013**, *5*, 3743–3749. http://dx.doi.org/10.1002/cctc.201300623
16. F. Nemati, M. M. Heravi, R. Saeedi Rad, *Chin. J. Catal.* **2012**, *33*, 1825–1831. http://dx.doi.org/10.1016/S1872-2067(11)60455-5
17. Q. Du, W. Zhang, H. Ma, J. Zheng, B. Zhou, Y. Li, *Tetrahedron.* **2012**, *68*, 3577–3584. http://dx.doi.org/10.1016/j.tet.2012.03.008
18. H. Yang, S. Li, X. Wang, F. Zhang, X. Zhong, Z. Dong, J. Ma, *J. Mol. Catal. A-Chem.* **2012**, *363–364*, 404–410. http://dx.doi.org/10.1016/j.molcata.2012.07.017
19. W. Li, B. Zhang, X. Li, H. Zhang, Q. Zhang, *Appl. Catal. A-Gen.* **2013**, *459*, 65–72. http://dx.doi.org/10.1016/j.apcata.2013.04.010
20. A. Hu, G. T. Yee, W. Lin, *J. Am. Chem. Soc.* **2005**, *127*, 12486–12487. http://dx.doi.org/10.1021/ja053881o
21. P. Wang, A. Kong, W. Wang, H.Y. Zhu, Y. K. Shan, *Catal Lett.* **2010**, *135*, 159–164. http://dx.doi.org/10.1007/s10562-010-0271-x
22. M. B. Gawande, A. K. Rathi, I. D. Nogueira, R. S. Varma, P.

S. Branco, *Green Chem.* **2013**, *15*, 1226–1231. http://dx.doi.org/10.1039/c3gc40375k

23. B. Atashkar, A. Rostami, B. Tahmasbi, *Catal. Sci. Technol.* **2013**, *3*, 2140–2146. http://dx.doi.org/10.1039/c3cy00190c

24. A. Alizadeh, M. M. Khodaei, M. Beygzadeh, D. Kordestani, M. Feyzi, *Bull. Korean Chem. Soc.* **2012**, *33*, 2546–2552. http://dx.doi.org/10.5012/bkcs.2012.33.8.2546

25. T. Zeng, L. Yang, R. Hudson, G. Song, A. R. Moores, C. Li, *Org. Lett.* **2011**, *13*, 442–445. http://dx.doi.org/10.1021/ol102759w

26. L. Weber, *Curr. Med. Chem.* **2002**, *9*, 2085–2093. http://dx.doi.org/10.2174/0929867023368719

27. G. Evano, N. Blanchard, M. Toumi, *Chem. Rev.* **2008**, *108*, 3054–3131. http://dx.doi.org/10.1021/cr8002505

28. V. Peres, T. J. Nagem, F. F. de Oliveira, *Phytochem.* **2000**, *55*, 683–710. http://dx.doi.org/10.1016/S0031-9422(00)00303-4

29. G. J. Bennett, H.-H. Lee, *Phytochem.* **1989**, *28*, 967–998. http://dx.doi.org/10.1016/0031-9422(89)80170-0

30. M. M. M. Pinto, M. E. Sousa, M. S. J. Nascimento, *Curr. Med. Chem.* **2005**, *12*, 2517–2538. http://dx.doi.org/10.2174/092986705774370691

31. R.-M. Ion, *Prog. Catal.* **1997**, *6*, 55–76.

32. C. G. Knight, T. Stephens, *Biochem. J.* **1989**, 258, 683–687. http://dx.doi.org/10.1042/bj2580683

33. S. M. Menchen, S. C. Benson, J. Y. L. Lam, W. Zhen, D. Sun, B. B. Rosenblum, S. H. Khan, M. Taing, U.S. Patent, US 6583168, 2003; *Chem. Abstr.* **2003**, *139*, 54287*f*.

34. M. Ahmad, T. A. King, K. Do-Kyeong, B. H. Cha, L. Jong-min, *J. Phys. D: Appl. Phys.* **2002**, *35*, 1473–1476. http://dx.doi.org/10.1088/0022-3727/35/13/303

35. D. Fang, J-M. Yang, Y-F. Cao, *Res. Chem. Intermed.* **2013**, *39*, 1745–1751. http://dx.doi.org/10.1007/s11164-012-0709-4

36. L-P. Mo, H.-L. Chen, *J. Chin. Chem. Soc.* **2010**, *57*, 157–161. http://dx.doi.org/10.1002/jccs.201000025

37. A. Zare, R. Khanivar, M. Hatami, M. Mokhlesi, M. A. Zolfigol, A. R. Moosavi-Zare, A. Hasaninejad, A. Khazaei, V. Khakyzadeh, *J. Mex. Chem. Soc.* **2012**, *56*, 389–394.

38. Z-H. Zhang, P. Zhang, S-H. Yang, H-J. Wang, J. Deng, *J. Chem. Sci.* **2010**, *122*, 427–432. http://dx.doi.org/10.1007/s12039-010-0049-0

39. R-Z. Wang, L-F. Zhang, Z-S. Cui, *Synth. Commun.* **2009**, *39*, 2101–2107. http://dx.doi.org/10.1080/00397910802638511

40. P. V. Shinde, A. H. Kategaonkar, B. B. Shingate, M. S. Shingare, *Beilstein J. Org. Chem,* **2011**, *7*, 53–58. http://dx.doi.org/10.3762/bjoc.7.9

41. Z. Hongjun, Z, Yong, C. Bowen, Z, Weiwei, X, Xianlin, R. Yuanlin, *Chin. J. Chem.* **2012**, *30*, 362–366.

42. J. M. Khurana, A. Lumb, A. Pandey, D. Magoo, *Synth. Commun.* **2012**, *42*, 1796–1803. http://dx.doi.org/10.1080/00397911.2010.544832

43. G. C. Nandi, S. Samai, R. Kumar, M.S. Singh, *Tetrahedron.* **2009**, *65*, 7129–7134. http://dx.doi.org/10.1016/j.tet.2009.06.024

44. X. J. Sun, J. F. Zhou, P. S. Zhao, *Synth. Commun.* **2012**, *42*, 1542–1549. http://dx.doi.org/10.1080/00397911.2010.541966

45. R. Mohammadi, E. Eidi, M. Ghavami, M. Z. Kassaee, *J. Mol. Catal. A-Chem.* **2014**, *393*, 309–316. http://dx.doi.org/10.1016/j.molcata.2014.06.005

46. M. A. Ghasemzadeh, J. Safaei-Ghomi, *Acta. Chim. Slov.* **2015**, *62*, 103–110.

47. J. Safaei-Ghomi, M. A. Ghasemzadeh, *J. Chem. Sci.* **2013**, *125*, 1003–1008. http://dx.doi.org/10.1007/s12039-013-0451-5

48. J. Safaei-Ghomi, M. A. Ghasemzadeh, *Acta. Chim. Slov.* **2012**, *59*, 697–702.

49. M. A. Ghasemzadeh, J. Safaei-Ghomi, S. Zahedi, *J. Serb. Chem. Soc.* **2013**, *78*, 769–779.

50. M. A. Ghasemzadeh, J. Safaei-Ghomi, H. Molaei, *C. R. Chimie.* **2012**, *15*, 969–974. http://dx.doi.org/10.1016/j.crci.2012.08.010

51. M. A. Ghasemzadeh, J. Safaei-Ghomi, *J. Chem. Res.* **2014**, *5*, 313–316. http://dx.doi.org/10.3184/174751914X13976454726953

52. J. Safaei-Ghomi, F. Eshteghal, M. A. Ghasemzadeh, *Acta. Chim. Slov.* **2014**, *61*, 703–708.

53. Y. Hu, Z. Zhang, H. Zhang, L. Luo, S.Yao, *J. Solid State Electro. Chem.* **2012**, *16*, 857–867. http://dx.doi.org/10.1007/s10008-011-1434-4

54. Y. H. Deng, D. W. Qi, C. H. Deng, X. M. Zhang, D. Y. Zhao, *J. Am. Chem. Soc.* **2008**, *130*, 28–29. http://dx.doi.org/10.1021/ja0777584

Povzetek

V raziskavi predstavljamo veliko uporabnost $Fe_3O_4@SiO_2$ nanodelcev z dvoslojno strukturo jedro-ovoj (»core-shell«) kot učinkovitih, zelenih, robustnih, cenovno ugodnih in večkrat uporabnih nanokatalizatorjev, primernih za pospešitev večkomponentne reakcije med aldehidi, 2-naftolom in dimedonom v zmesi etanola in vode kot topila pod pogoji refluksa. V opisanem postopku smo se uspeli izogniti uporabi nevarnih reagentov in topil in zato lahko to metodo označimo kot zeleno alternativo ostalim metodam. Enostavnost postopka, neškodljivost okolju, odlični izkoristki, kratki reakcijski časi, enostavnost izolacije in čiščenja so glavne odlike tega protokola. Karaketrizacija in določitev strukture pripravljenih produktov je bila izvedena na osnovi kemijskih, analitskih in spektralnih analiz. Heterogene nanodelce smo natančno karakterizirali tudi na osnovi FT-IR, XRD, EDX, VSM in SEM analiz.